An integrated portable system for single chip simultaneous measurement of multiple disease associated metabolites

Samadhan B. Patil[a],[*], Dharmendra S. Dheeman[b],[1], Mohammed A. Al-Rawhani[a],
Srinivas Velugotla[a], Bence Nagy[a], Boon Chong Cheah[a], James P. Grant[a], Claudio Accarino[a],
Michael P. Barrett[b], David R.S. Cumming[a],[*]

[a] Electronics and Nanoscale Engineering, School of Engineering, University of Glasgow, Glasgow G12 8LT, United Kingdom
[b] Wellcome Centre for Molecular Parasitology, Institute of Infection, Immunity and Inflammation, University of Glasgow, Glasgow G12 8TA, United Kingdom

ARTICLE INFO

ABSTRACT

Metabolites, the small molecules that underpin life, can act as indicators of the physiological state of the body when their abundance varies, offering routes to diagnosis of many diseases. The ability to assay for multiple metabolites simultaneously will underpin a new generation of precision diagnostic tools. Here, we report the development of a handheld device based on complementary metal oxide semiconductor (CMOS) technology with multiple isolated micro-well reaction zones and integrated optical sensing allowing simultaneous enzyme-based assays of multiple metabolites (choline, xanthine, sarcosine and cholesterol) associated with multiple diseases. These metabolites were measured in clinically relevant concentration range with minimum concentrations measured: $25\,\mu M$ for choline, $100\,\mu M$ for xanthine, $1.25\,\mu M$ for sarcosine and $50\,\mu M$ for cholesterol. Linking the device to an Android-based user interface allows for quantification of metabolites in serum and urine within 2 min of applying samples to the device. The quantitative performance of the device was validated by comparison to accredited tests for cholesterol and glucose.

1. Introduction

Many diseases are accompanied by perturbations to normal levels of the small molecules collectively called "metabolites" within biofluids. As our ability to identify and quantify multiple small molecules has improved in recent years, it has become clear that many diseases are characterised by differences in metabolite levels (Asiago et al., 2010; Griffin et al., 2011; Griffin and Shockcor, 2004; Guo et al., 2015; Mazzu-Nascimento et al., 2016; Mendrick and Schnackenberg, 2009; Nicholson et al., 2012; Sreekumar et al., 2009; Sullivan et al., 2016; Sun et al., 2013). Metabolomics technologies that aim to measure all small molecules in a given system have been at the centre of this increased appreciation of metabolite biomarkers of disease. Metabolomics usually involves one of two platforms to profile metabolites: nuclear magnetic resonance (NMR) and mass spectrometry coupled to liquid or gas chromatographic separation systems e.g. (LC/GC-MS). NMR based measurements are highly quantitative, but suffer from a relative lack of sensitivity, with only the most abundant molecules visible (Malet-Martino and Martino, 1991). Hyphenated mass spectrometry based

approaches are far more sensitive and cover a greater range of metabolites, but lack the ability to quantify metabolites without additional steps in the analytical process (Fernie et al., 2004). In both cases the basic instrumentation is expensive and not suitable for point-of-care (POC) analysis. New methodologies are required if metabolomics is to be democratised, hence novel ways of measuring multiple metabolites simultaneously are required. Complementary metal oxide semiconductor (CMOS) technology, the mainstay of low-cost electronics, has proven to be of great utility in allowing coupling of many biological processes to electronic measurement (Abbott et al., 2017; Bellin et al., 2016; Piliarik and Sandoghdar, 2014). Exploiting CMOS technology to provide new scalable metabolite measurement platforms also shows excellent potential. An approach to metabolite measurement that can be applied to CMOS technology involves enzymes capable of recognising particular metabolites. Enzymes have exquisite sensitivity for their metabolite substrates that can be quantified based on the rate at which they are reacted upon by enzymes. Because of the ultra-high packing density of CMOS based sensors, this technology has the capacity to interrogate a large number of biochemical reactions provided

surface engineering can keep reactions discrete. Enzyme reactions can be followed using detection systems capable of integration into a CMOS circuit enabling selective measurement of metabolites in bodily fluids placed on a chip's surface. Both individual as well as simultaneous measurement of glucose and cholesterol have been demonstrated on a semiconductor platform (Al-Rawhani et al., 2017; Cheah et al., 2016; Hu et al., 2017). Similarly, immunoassays have also been demonstrated (Nagy et al., 2018). In principle, a multitude of enzymes, each specific for a given metabolite, could be multiplexed onto the same CMOS-chip surface, scaling to a point where as many metabolites for which enzymes are available could potentially be measured simultaneously.

The ability to detect and quantify multiple metabolite biomarkers simultaneously and rapidly can be of the utmost importance for the critical disease conditions such as acute myocardial infarction and acute ischaemic stroke. Immediate application of the most appropriate therapeutic management can greatly improve outcomes in these diseases (Neumann et al., 2016; Rothwell et al., 2007). In many cancers too, it is becoming clear that therapeutic choices based on metabolite profiles offer improved outcomes (Puchades-Carrasco and Pineda-Lucena, 2017). In this article, we present a handheld device for the simultaneous rapid detection and quantification of a representative panel of multiple metabolites: choline (Adamczyk et al., 2006; Danne et al., 2003; Danne and Möckel, 2010; Wang et al., 2011); xanthine (Chouchani et al., 2014; Dawson and Walters, 2006; Farthing et al., 2015; Harmsen et al., 1981); sarcosine (Cernei et al., 2013; Mazzu-Nascimento et al., 2016; Sreekumar et al., 2009; Wang et al., 2017); and cholesterol (Holmes et al., 2017). Each of these metabolites has been implicated in one or more critical disease states such as acute ischaemia (for heart or brain), acute renal failure and prostate cancer, thus demonstrate the feasibility and purpose of simultaneously quantifying multiple metabolites on a single chip (Danne and Möckel, 2010; Farthing et al., 2015; Holmes et al., 2017; Li et al., 2015; Sreekumar et al., 2009). Metabolite-specific enzyme assays used with an array of sensors based on CMOS technology has enabled this multiplexed metabolite measurement. The CMOS-chip surface consists of a 16×16 pixel array divided into four discrete micro-wells, one for each specific metabolite, thus enabling rapid simultaneous detection of multiple metabolites. This simple device is operable using any Android based tablet or smartphone that provides data acquisition, computation, visualisation and power through a USB connector.

2. Materials and methods

2.1. CMOS-chip design

A $3.4\,mm \times 3.6\,mm$ chip was designed and fabricated using an Austria microsystems (AMS) 350 nm triple-well process. This chip has 16×16 array of sensor pixels with an active area of $1.6\,mm \times 1.6\,mm$ and was designed using Cadence Virtuoso software package.

2.2. Fabrication of micro-wells

The active area surface of a CMOS-chip, with pixel array for the sensors, was protected by four polydimethylsiloxane (PDMS) micro-blocks of $600\,\mu m \times 600\,\mu m$ and height of $1500\,\mu m$ (SYLGARD 184 Silicone Elastomer Kit, Dow Corning). These PDMS blocks serve two purposes: (1) they act as a sacrificial material helping shape the micro-casting of black epoxy (EPO-TEC 302–3M Black Kit, Epoxy Technology Inc.) to fabricate the micro-wells, and (2) they also protect the active pixel array area of CMOS-chip against damage from epoxy or from physical damage through scratches. Cast PDMS used in this process was never older than 14 h. These PDMS blocks were carefully placed on top of the active pixel array using the assistive translation stage of a flip-

chip bonder (Semiconductor Equipment Corporation, Model 850). The epoxy mixture was carefully decanted over the CMOS-chip surface around the PDMS blocks and over the contact pads. Overnight curing at a maximum temperature of 60 °C caused the epoxy resin to harden. A clear plastic ring of approximately 8 mm height was placed around the CMOS-chip on a ceramic chip carrier to form a reaction cell. Four quadrant separation walls were made using selective micro-cavity casting of black epoxy (Fig. S1, Supplementary Information). These micro-wells have pipettable access. This unique design does not require micro-tubing or pumps to handle the liquid, avoiding complex liquid handling. The method also allows instantaneous mixing of reagents with micro-wells, reducing the assay time by avoiding fluid travel delays that micro-tubing would introduce.

2.3. On-chip metabolite assays

The assay reagents and the commercially available enzymes used were from Sigma-Aldrich Company Ltd. (Dorset, UK). The enzymes, choline oxidase (CHOD) from *Alcaligenes* sp., xanthine oxidase (XOD) from *Escherichia coli* K-12, sarcosine oxidase (SOX) from *Bacillus* sp., cholesterol esterase from *Pseudomonas* sp., cholesterol oxidase (COD) from *Streptomyces* sp., glucose oxidase (GOD) from *Aspergillus niger*, and horseradish peroxidase (HRP) from *Amoracia rusticana* roots, were all obtained as lyophilised powders, which were reconstituted in their respective assay buffers before on-chip assays. The sterile-filtered serum sample used was from human male AB plasma (Sigma-Aldrich) and the urine sample used was obtained from a local volunteer. An assay mixture of 500 μl was used for on-chip assays to effectively cover the active chip sensor array as well as the surrounding surface within the chip-enclosure ring.

2.3.1. Choline

An enzymatic assay based on CHOD was employed to measure choline (Hiroaki et al., 1977; Keesey, 1987). The assays were performed in 100 mM Tris-HCl buffer (pH 8.0) and diluted serum using 2.5 units (U) of CHOD, where choline was oxidised to betaine with the simultaneous production of hydrogen peroxide (H_2O_2). The formed H_2O_2 was measured on a CMOS-Photodiode (PD) sensor array (Fig. 2d) using a phenol/4-aminoantipyrine/HRP coupled reaction system to produce quinoneimine dye (λ_{max} at 553 nm) (Rautela and Liedtke, 1978). Choline concentration in the assays was varied from 25 μM to 500 μM.

2.3.2. Xanthine

An enzymatic assay based on XOD was employed to measure xanthine (Roussos, 1967). The assays were performed in 50 mM triethanolamine buffer (pH 7.5) and diluted serum using 2.0 U of XOD, where xanthine was oxidised to uric acid with the simultaneous production of H_2O_2. The formed H_2O_2 was measured on a CMOS-PD sensor array using a phenol/4-aminoantipyrine/HRP coupled reaction system to produce quinoneimine dye (Rautela and Liedtke, 1978). Xanthine concentration in the assays was varied from 100 μM to 1.6 mM.

2.3.3. Sarcosine

An enzymatic assay based on SOX was employed to measure sarcosine (Suzuki, 1981). Sarcosine assays were performed in 60 mM glycylglycine buffer (pH 8.3) and diluted urine using 4.1 U of SOX, where sarcosine was oxidised to glycine and formaldehyde with the simultaneous production of H_2O_2. The formed H_2O_2 was measured on a CMOS-PD sensor array using an o-dianisidine/HRP coupled reaction system to produce oxidised o-dianisidine (λ_{max} at 540 nm) (Porstmann et al., 1981). Sarcosine concentration in the assays was varied from 1.25 μM to 10 mM.

2.3.4. Cholesterol

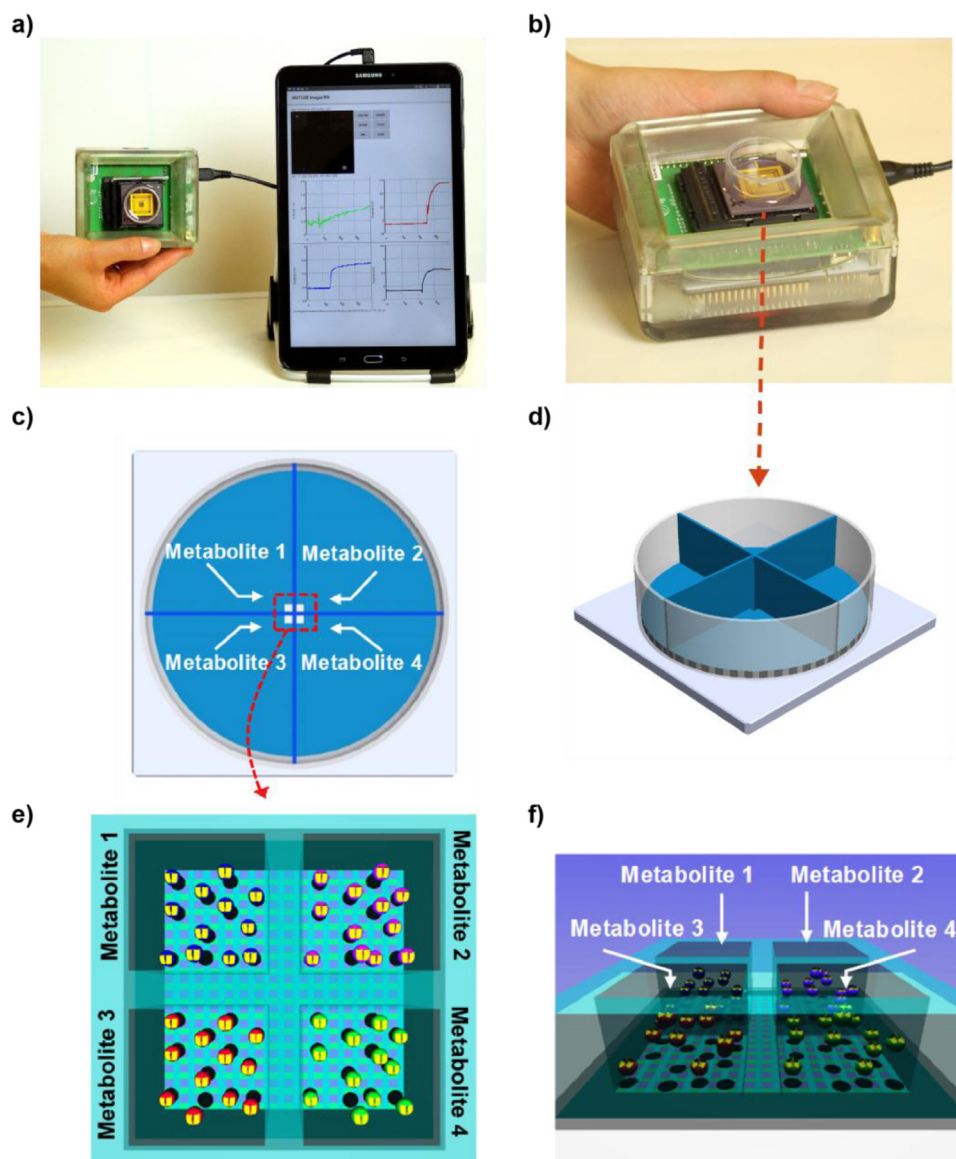An enzymatic assay based on COD was employed to measure

Fig. 1. A handheld prototype for the multiplexed assaying of metabolites. (**a**) Prototype consisting of a post-processed CMOS-chip with electronic readout attached to an Android-based tablet for data acquisition. (**b**) The handheld device with CMOS-chip. (**c**) Top-view of a fluid retaining ring bonded on to the ceramic chip carrier with the micro-well structure at the centre. (**d**) Side-view of the packaged structure. (**e**) A more detailed top-view of the micro-well structure over the chip. (**f**) Side-view, showing isolated reaction zones for assaying of four different metabolites with specific enzymes in individual micro-wells.

cholesterol (Amundson and Zhou, 1999). Cholesterol assays were performed in 50 mM triethanolamine buffer (pH 7.5) and diluted serum with 1.2 U of COD, where cholesterol esterase-treated (~30 min at 37 °C) cholesterol was oxidised to a ketone product (5-cholesten-3-one) with the simultaneous production of H_2O_2. The formed H_2O_2 was measured on a CMOS-PD sensor array using an o-dianisidine/HRP coupled reaction system to produce oxidised o-dianisidine. Cholesterol concentration in the assays was varied from 50 μM to 870 μM.

2.3.5. Glucose

An enzymatic assay based on GOD was employed to measure glucose (Washko and Rice, 1961). Glucose assays were performed in 50 mM triethanolamine buffer (pH 7.5) and diluted serum with 1.2 U of GOD, where glucose was oxidised to a lactone (D-glucono-1,5-lactone) with the simultaneous production of H_2O_2. The formed H_2O_2 was measured on a CMOS-PD sensor array using an o-dianisidine/HRP coupled reaction system to produce oxidised o-dianisidine. Glucose concentration in the assay was varied from 700 μM to 5.6 mM.

2.3.6. Calculation of the rates

The rates were estimated from the slope of the tangent drawn to the portion of the curve representing the initial rate (Purich, 2010). For the determination of the calibration curves, the background rates due to the presence of endogenous serum metabolites were subtracted from the rates obtained for the serum samples to which known quantities of metabolite were added.

2.4. Android-based data acquisition application

An Android data acquisition Application was developed for the multiplexed sensing. The App displays the data acquired from the sensor array in three different formats: a greyscale image; 4 time domain graphs of selected pixels; and a bar chart showing current signal levels of the selected pixels. The application triggers the platform to send a data frame at the rate of 10 frames per second, which can be adjusted in the source code. The acquired data can be stored into a .CSV file for later analysis.
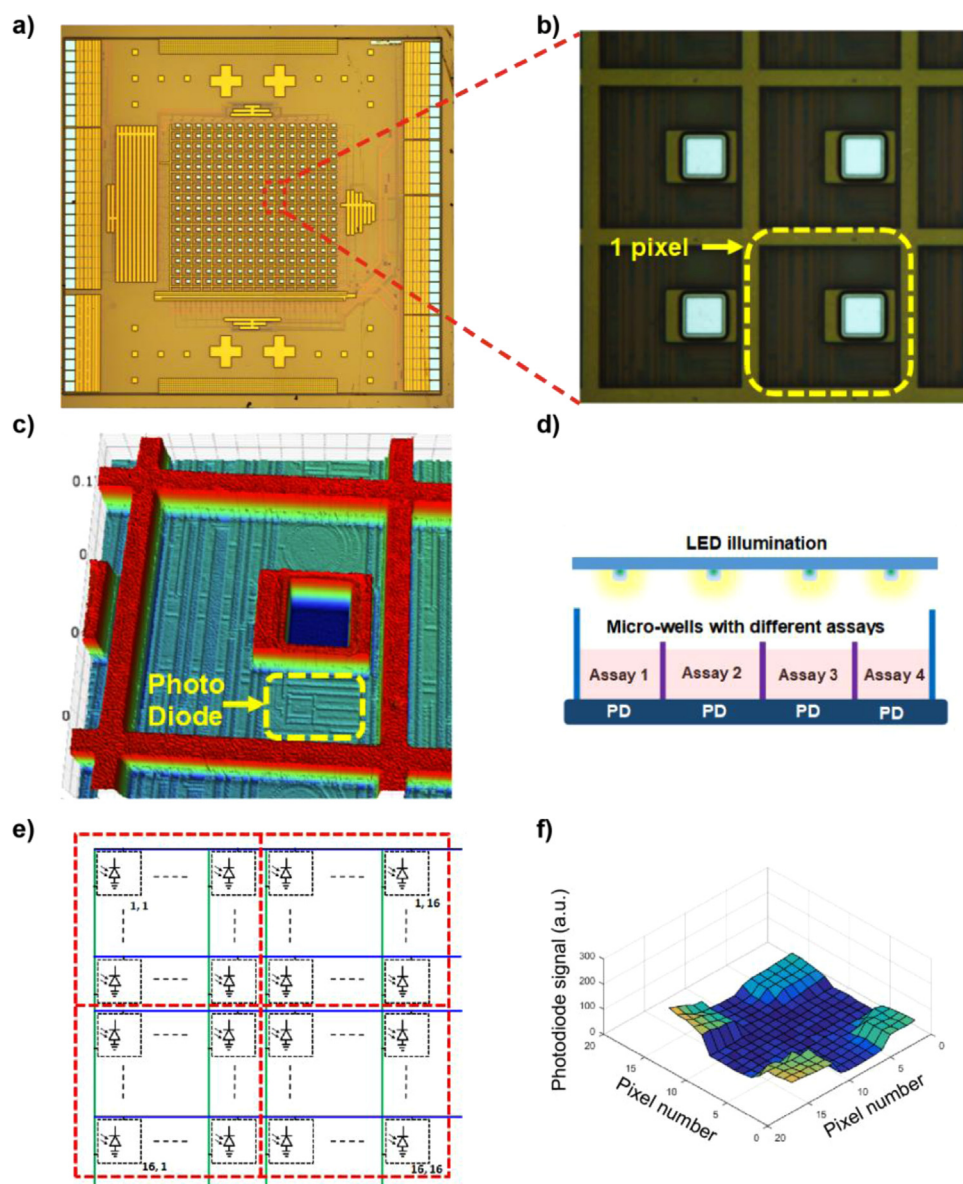
Fig. 2. CMOS-chip architecture. (**a**) CMOS-chip with a 16 × 16 array of sensor pixels. (**b**) Magnified view of a CMOS-chip with a dashed square showing a single sensor pixel. (**c**) An optical profilometry micrograph of a single CMOS-chip sensor pixel showing a photodiode. (**d**) Schematic depiction of the sensing principle employed for metabolite sensing in four micro-wells using light-emitting diodes (LED) and photodiode (PD) sensors. (**e**) Schematic of a CMOS-chip circuit showing the division of a 16 × 16 pixel array into four micro-wells. The micro-well boundaries are shown by dashed lines. (**f**) Photodiode signal from the four micro-wells, shown as a surface plot, acquired during simultaneously assays for four metabolites.

3. Results and discussion

3.1. A handheld multi-metabolite measuring CMOS-based platform

A CMOS based hand held device developed for the simultaneous, rapid detection and quantification of multiple metabolite biomarkers is presented (Figs. 1a and 1b). Metabolites were detected using assays within discrete micro-wells; one for each metabolite (Fig. 1c-f) whose concentrations in blood or urine vary with differing types of diseases. The device demonstrates the potential to create a new miniaturised approach to metabolomic analysis. The CMOS 16 × 16 pixel array is shown in Figs. 2a and 2b. Each pixel consists of a photodiode (Figs. 2b and 2c). The chip was designed and fabricated using an Austria microsystems (AMS) 350 nm triple-well process that allowed the sensors to be isolated from each other to achieve minimum cross talk. The photodiode has a measured peak responsivity of 21.6 mV/μW at a wavelength of 600 nm (Fig. S2, Supplementary Information). The surface of the CMOS-chip was post-processed and partitioned to create micro-wells on the chip surface. These micro-wells were fabricated using additive epoxy micro-casting using PDMS as a sacrificial layer (see Section 2.2). Figs. 1c and 1d provide a schematic view for the post-

processed packaged CMOS-chip with micro-wells in the centre of the package. These micro-wells form isolated reaction zones, each for an individual metabolite biomarker (Figs. 1e and 1f) using enzyme-based assays to detect four different metabolites.

Enzymes that produce H_2O_2 can be coupled to reactions offering an assay that exhibits a colour change; in this work we achieve this through coupling to HRP. Such a coupled colorimetric assay can be monitored in real time using a photodiode. As illustrated in Fig. 2d the photodiode array integrated in a CMOS platform can, therefore, be used for the quantification of metabolites based on the incident light intensity after transmission through the respective assay solutions. After fabrication, each micro-well has an array of approximately 5 × 5 pixels with photodiodes to sense the reaction and to provide a statistically averaged output signal over the micro-well area as shown in Fig. 2e. A typical output signal from individual photodiode pixels across the entire CMOS-chip is shown in Fig. 2f. The spatial surface plot for the signal exhibits the distinct reaction zones of each micro-well and assay. A standard deviation of output signal for a CMOS-chip with different numbers of reaction wells was evaluated (Fig. S3, Supplementary Information).
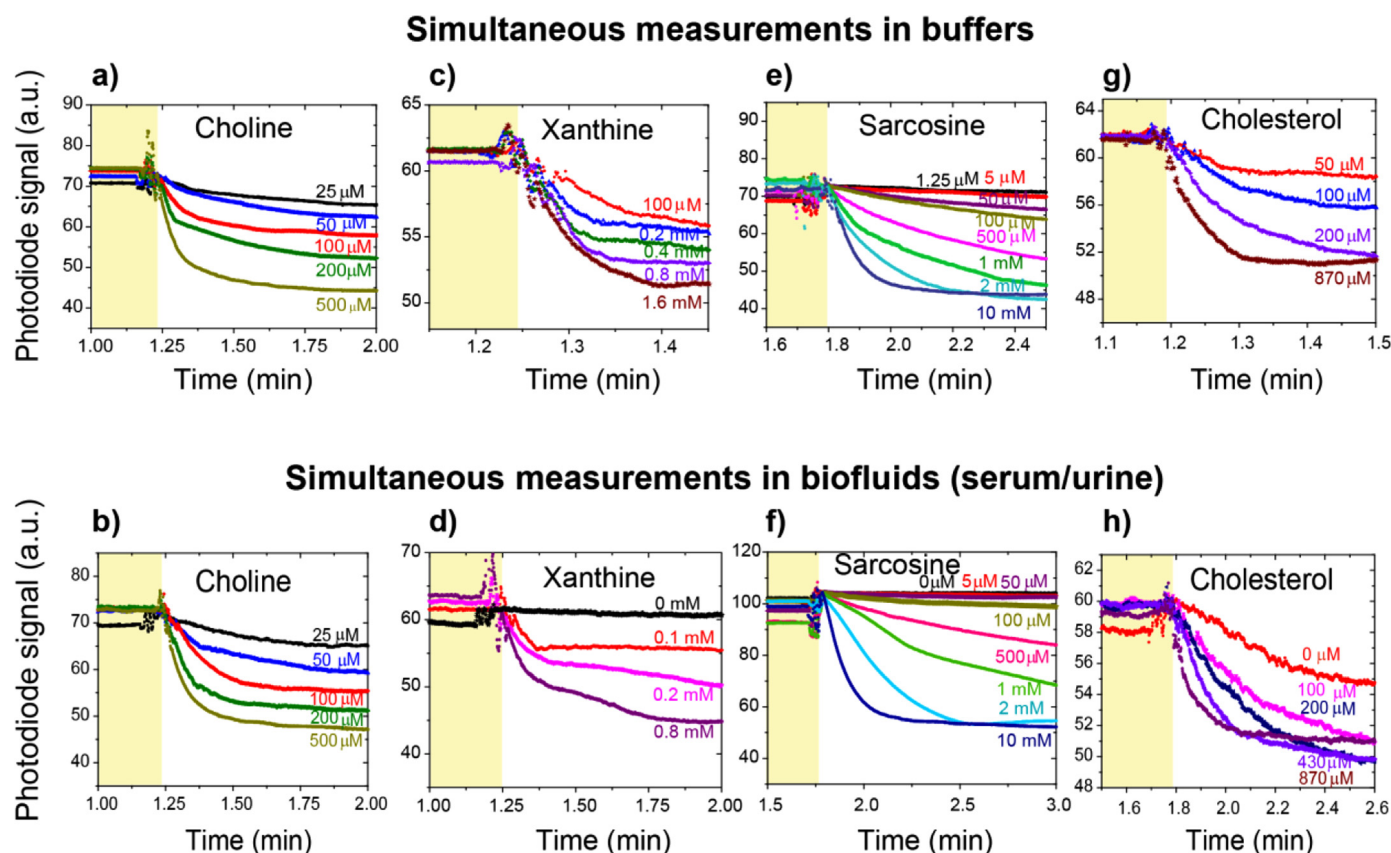
Simultaneous measurements in buffers

Simultaneous measurements in biofluids (serum/urine)

Fig. 3. Response of photodiode sensor array from four micro-wells for simultaneous detection of four different metabolites. (**a**) Photodiode response for the detection of choline in buffer with concentrations varied from 25 μM to 500 μM. (**b**) Photodiode response for the detection of choline in diluted serum, with concentrations varied from 25 μM to 500 μM. (**c**) Photodiode signal response for the detection of xanthine in buffer with concentrations varied from 100 μM to 1.6 mM. (**d**) Photodiode signal response for the detection of xanthine in diluted serum, with the concentrations varied from 0.1 mM to 0.8 mM. (**e**) Photodiode signal response for the detection of sarcosine in buffer with concentrations varied from 1.25 μM to 10 mM. (**f**) Photodiode signal response for the detection of sarcosine in diluted urine, with concentrations varied from 5 μM to 10 mM. (**g**) Photodiode signal response for the detection of cholesterol in buffer with concentrations varied from 50 μM to 870 μM. (**h**) Photodiode signal response for the detection of cholesterol in diluted serum, with the concentrations varied from 100 μM to 870 μM. Photodiode signals are given in arbitrary units (a. u.) since the offset in the initial value for each measurement has been manually removed for ease of comparison in the graphs, hence data values are not absolute. The numerical variation in signal is measured in millivolts (mV) in every case.

3.2. Identification of individual and multiple metabolites

Measurements were carried out on metabolites dissolved in various solvents including buffer, serum and urine using enzymes specific for a range of metabolites. Assays for these metabolites were optimised, standardised and quantified on the CMOS-chip surface either one at a time or in pairs across the micro-wells to record statistical variation.

The choline level in serum is emerging as a biomarker to detect early onset of troponin-positive cardiac ischaemia (Danne et al., 2003; Danne and Möckel, 2010; Wang et al., 2011), where levels of 20–60 μM are reported in comparison to concentrations in a healthy individuals of around 10 μM (Adamczyk et al., 2006; Danne et al., 2003; Danne and Möckel, 2010). We employed a colorimetric coupled assay based on CHOD generated H_2O_2 for detection and quantification of choline. To assess the linear dynamic range for choline on the CMOS platform, we measured choline in buffer and also in the presence of diluted serum over a concentration range of 25–500 μM (Fig. 3**a-b**). We were able to reliably detect the lowest choline concentration of 25 μM which would be detectable in diseased but not healthy individuals.

Xanthine oxidase and its specific metabolite substrates, xanthine and hypoxanthine, have also been recognised as biomarkers for ischaemia (Ali et al., 2013; Chouchani et al., 2014; Farthing et al., 2015), as well as for other diseases including acute renal failure (Bradbury et al., 1995). Here, we used a colorimetric coupled assay based on XOD generated H_2O_2 for the detection and quantification of

xanthine, both in buffer (Fig. 3**c**) and in diluted serum (Fig. 3**d**) over a concentration range from 100 μM to 1.6 mM.

Sarcosine, a non-proteinogenic amino acid metabolite, has normal levels of around 0.02 μM in urine samples of healthy individuals. Elevated levels of sarcosine were observed in urine during progression and metastasis of prostate cancer and can reach elevated levels of ~5 μM (Cernei et al., 2013). We successfully measured sarcosine, using a colorimetric coupled assay based on SOX generated H_2O_2, in buffer over a concentration range of 1.25 μM to 10 mM (Fig. 3**e**) and also in diluted urine (Fig. 3**f**) down to a concentration of 5 μM.

3.3. On-chip enzyme kinetics and validation of CMOS device

Validation of the on-chip assays for the 4-assay system was carried out using similar protocols to those used in single assay chips (Al-Rawhani et al., 2017; Hu et al., 2017). Details of the work done using the present 4-assay system are provided in the Supplementary Information (Section 4, Fig. S4).

Measurements were carried out to obtain on-chip kinetics in buffer and diluted serum, for choline, xanthine, sarcosine, and cholesterol. Fig. 3**g-h** and Figs. S4a-b (see Supplementary Information) show that there was a metabolite concentration-dependent change in the sensor response. Control reactions showed no response or showed a response equivalent to the endogenous metabolite concentration in the diluted serum (shaded part of the curves in the Fig. 3**g-h** and Figs. S4a-b). In
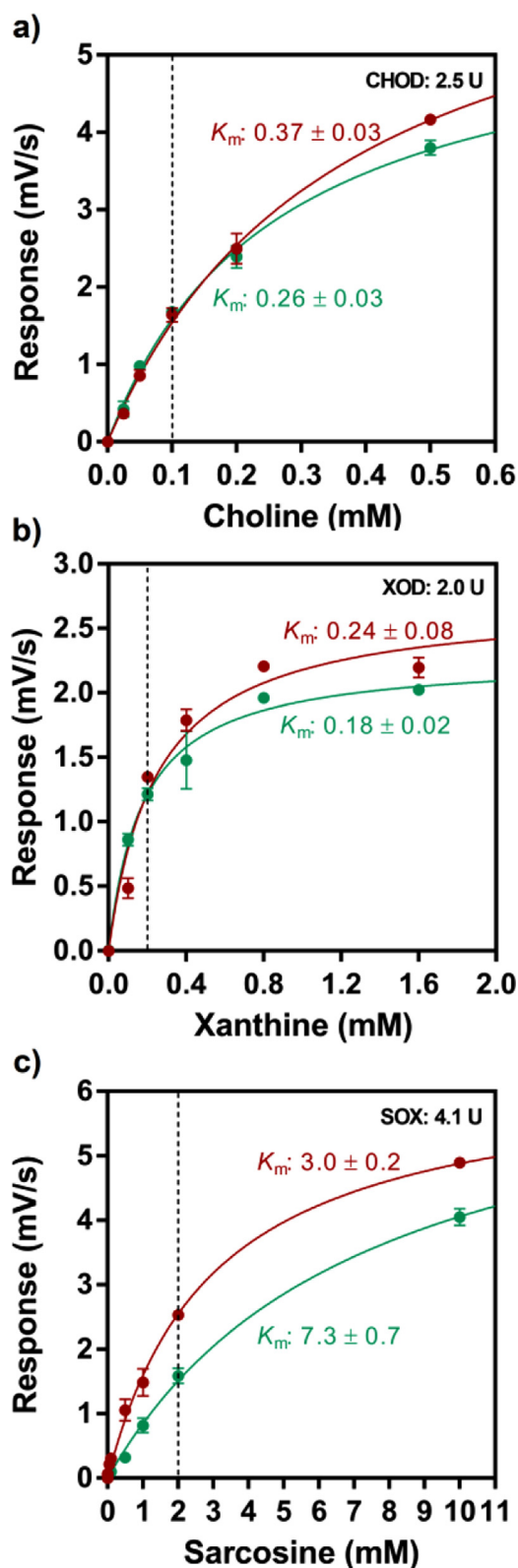
Fig. 5. The validation of handheld CMOS device. The plot depicts the measured values of glucose and cholesterol using two independent quantification methodologies. The same human serum sample was tested at NHS on an Abbott ARCHITECT clinical chemistry analyser ($n = 8$) and by our handheld CMOS-based device ($n = 4$). The statistical difference between the two groups of determined values was evaluated using a Student unpaired t-test. There is no statistically significant difference between the two groups of measurements as indicated by the p values (> 0.05).

Fig. 4. On-chip kinetic analysis using photodiode sensor array. (**a**) Initial rates for choline in buffer (red) and in diluted serum (green), with concentrations varied from 25 µM to 500 µM. (**b**) Initial rates for xanthine in buffer (red) and in diluted serum (green), with concentrations varied from 0.1 mM to 1.6 mM and 0.1–0.8 mM, respectively. (**c**) Initial rates for sarcosine in buffer (red) and in diluted urine (green), with concentrations varied from 1.25 µM to 10 mM and 5 µM to 10 mM, respectively. The dashed lines in the kinetics curves depict the linear dynamic range for on-chip assay in the diluted serum. The data shown are the mean of independent experiments ($n = 4$) and the error bars show the standard error of the mean (SEM).
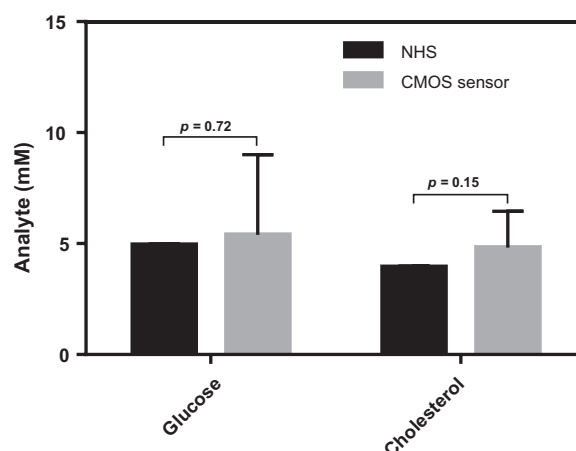
order to use the system quantitatively, variation in measured activity (transduced into biosensor response) must be a function of the metabolite-substrate concentration and thus the metabolite-substrate needs to be within a linear operable range, near or below the Michaelis constant (K_m) of the metabolite-specific enzyme. This property of the enzyme ultimately dictates the linear dynamic range of the biosensor (Chica et al., 2005). The biosensor response was found to be metabolite concentration-dependent, showing a typical Michaelis-Menten kinetics with a distinct dynamic range, indicated by the dashed line, for the quantification of each metabolite in the diluted serum (Fig. 4**a-c** and Figs. S4c-d). The CHOD employed here exhibited a K_m of 0.37 mM in buffer and 0.26 mM in the presence of diluted serum (Fig. 4**a**); thus the choline biosensor operates well below substrate saturation levels in the linear dynamic range up to 100 µM of choline. The XOD used here showed a K_m of 0.24 mM and 0.18 mM in buffer and diluted serum, respectively (Fig. 4**b**). The xanthine biosensor too, therefore operates well below substrate saturation in the linear dynamic range of xanthine up to 200 µM. The concentration of sarcosine in urine of normal human subjects is approximately 0.02 µM which has been reported to increase up to 5 µM in the patients with prostate cancer (Cernei et al., 2013). The SOX used here showed a K_m in buffer of 3 mM and in diluted urine of 7.3 mM (Fig. 4**c**); hence the sarcosine biosensor also operates well below substrate saturation in the linear dynamic range up to 2 mM sarcosine with the lowest detectable concentration of 1.25 µM, thus reaching detectable levels in patients.

To validate our CMOS device, we investigated the detection of two commonly used metabolites, cholesterol and glucose, which are markers for the risk of cardiovascular disease and diabetes respectively. Similar peroxidase coupled colour reactions were adopted and monitored in real time using photodiode sensors (Fig. S4a-d). The accuracy of the values obtained using the CMOS-based device was validated by comparison of unknown serum values measured against UK NHS laboratory certified measurements for glucose and cholesterol on an Abbott ARCHITECT clinical chemistry analysis platform (Abbott, Illinois, USA). These assays were carried out, using enzymatic methods, for the same serum sample. The bar chart (Fig. 5) depicts the measured values for glucose and cholesterol using the two independent quantification methodologies (metabolites measured in the ARCHITECT system and CMOS-based device). There was no statistically significant difference between the two groups of measurements as indicated by the

p values ($>$ 0.05 using Student unpaired *t*-test). These results indicate that our CMOS-based device can reliably quantify these metabolites in clinical samples. In addition, this technology offers the advantage of performing multiplexed detection of different analytes covering metabolomic and immunological biomarkers (Nagy et al., 2018).

Having demonstrated each of the target assays, and obtained verification that glucose and cholesterol levels were well matched to available NHS assays, we then showed that we could assay four metabolites simultaneously using this handheld platform. A movie of real time outputs is shown in the Supplementary Information (Fig. S5; **Movie Clip 1**) demonstrating successful detection of all four metabolites together.

This ability of a CMOS based platform to detect and quantify choline, xanthine, sarcosine and cholesterol simultaneously, with an assay time of just 2 min, demonstrates new potential for a rapid POC platform for diagnosing multiple diseases using metabolite profiling. The successful simultaneous quantification of multiple metabolites also points to the feasibility of scaling this technology to measure a wider range of metabolites, capable of diagnosing many diseases as their metabolic perturbations become evident.

4. Conclusions

We have developed a handheld device based on CMOS technology capable of quantifying multiple metabolites choline, xanthine, sarcosine, and cholesterol simultaneously using specific enzymes. These metabolites, proposed as potential biomarkers for acute ischaemia (for heart or brain), acute renal failure and prostate cancer, were detected in less than 2 min offering the potential to use this handheld device in clinical and non-clinical settings. Furthermore, the biosensor performance was validated for measurement accuracy using glucose and cholesterol by comparison to NHS certified tests for the same metabolites. All of these measurements are conducted using an autonomous handheld device based on chip-based technology integrated into a mobile handheld unit. Having demonstrated the ability to measure multiple metabolites simultaneously we are now in a position to scale up the numbers of enzymes applied to the chip surface with a long-term aim of generating arrays suitable for diagnosing any disease for which metabolic perturbations are known. The technology has general applicability in primary and personal care settings, alleviating the burden on healthcare provision world-wide. We expect future versions of the technology to embed microfluidic sample handling and enzyme immobilisation (Sunayama and Takeuchi, 2014) to remove the need for off-chip sample preparation.

Acknowledgement

Appendix A. Supporting information

Supplementary data associated with this article can be found in the online version at doi:10.1016/j.bios.2018.09.013.

References

Abbott, J., Ye, T., Qin, L., Jorgolli, M., Gertner, R.S., Ham, D., Park, H., 2017. Nat. Nanotechnol. 12, 460–466.

Adamczyk, M., Brashear, R.J., Mattingly, P.G., 2006. Clin. Chem. 52, 2123–2124.

Al-Rawhani, M.A., Cheah, B.C., Macdonald, A.I., Martin, C., Hu, C., Beeley, J., Gouveia, L.C., Grant, J.P., Campbell, G., Barrett, M.P., Cumming, D.R.S., 2017. IEEE Sens. J. 17, 240–247.

Ali, O.S., Abdelgawad, H.M., Mohammed, M.S., El-Awady, R.R., 2013. Heart Vessels 29, 629–637.

Amundson, D.M., Zhou, M., 1999. J. Biochem. Biophys. Methods 38, 43–52.

Asiago, V.M., Alvarado, L.Z., Shanaiah, N., Gowda, G.A.N., Owusu-Sarfo, K., Ballas, R.A., Raftery, D., 2010. Cancer Res. 70, 8309–8318.

Bellin, D.L., Sakhtah, H., Zhang, Y., Price-Whelan, A., Dietrich, L.E.P., Shepard, K.L., 2016. Nat. Commun. 7, 10535.

Bradbury, M.G., Henderson, M., Brocklebank, J.T., Simmonds, H.A., 1995. Pediatr. Nephrol. 9, 476–477.

Cernei, N., Heger, Z., Gumulec, J., Zitka, O., Masarik, M., Babula, P., Eckschlager, T., Stiborova, M., Kizek, R., Adam, V., 2013. Int. J. Mol. Sci. 14, 13893–13908.

Cheah, B.C., MacDonald, A.I., Martin, C., Streklas, A.J., Campbell, G., Al-Rawhani, M.A., Nemeth, B., Grant, J.P., Barrett, M.P., Cumming, D.R.S., 2016. IEEE Trans. Biomed. Circuits Syst. 10, 721–730.

Chica, R.A., Doucet, N., Pelletier, J.N., 2005. Current Opinion in Biotechnology 16, 378–384.

Chouchani, E.T., Pell, V.R., Gaude, E., Aksentijević, D., Sundier, S.Y., Robb, E.L., Logan, A., Nadtochiy, S.M., Ord, E.N.J., Smith, A.C., Eyassu, F., Shirley, R., Hu, C.-H., Dare, A.J., James, A.M., Rogatti, S., Hartley, R.C., Eaton, S., Costa, A.S.H., Brookes, P.S., Davidson, S.M., Duchen, M.R., Saeb-Parsy, K., Shattock, M.J., Robinson, A.J., Work, L.M., Frezza, C., Krieg, T., Murphy, M.P., 2014. Nature 515, 431–435.

Danne, O., Möckel, M., 2010. Expert Rev. Mol. Diagn. 10, 159–171.

Danne, O., Möckel, M., Lueders, C., Mügge, C., Zschunke, G.A., Lufft, H., Müller, C., Frei, U., 2003. Am. J. Cardiol. 91, 1060–1067.

Dawson, J., Walters, M., 2006. Br. J. Clin. Pharmacol. 62, 633–644.

Farthing, D.E., Farthing, C.A., Xi, L., 2015. Exp. Biol. Med. 240, 821–831.

Fernie, A.R., Trethewey, R.N., Krotzky, A.J., Willmitzer, L., 2004. Nat. Rev. Mol. Cell Biol. 5, 763–769.

Griffin, J.L., Atherton, H., Shockcor, J., Atzori, L., 2011. Nat. Rev. Cardiol. 8, 630–643.

Griffin, J.L., Shockcor, J.P., 2004. Nat. Rev. Cancer 4, 551–561.

Guo, L., Tan, G., Liu, P., Li, H., Tang, L., Huang, L., Ren, Q., 2015. Sci. Rep. 5, 15126.

Harmsen, E., Jong, J.W., de, Serruys, P.W., 1981. Clin. Chim. Acta 115, 73–84.

Hiroaki, O., Kazuyo, S., Nobuyuki, N., Akio, N., 1977. Clin. Chim. Acta 80, 87–94.

Holmes, M.V., Ala-Korpela, M., Smith, G.D., 2017. Nat. Rev. Cardiol. 14, 577–599.

Hu, C., Al-Rawhani, M., Cheah, B.C., Velugotla, S., Cumming, D.R.S., 2017. IEEE Sens. J. 18, 484–493.

Keesey, J., 1987. Biochemica information, 1st ed. Boehringer Mannheim Biochemicals, Indianapolis, 19-20.

Li, L., Wang, Y., Pan, L., Shi, Y., Cheng, W., Shi, Y., Yu, G., 2015. Nano Lett. 15, 1146–1151.

Malet-Martino, M.-C., Martino, R., 1991. Clin. Pharmacokinet. 20, 337–349.

Mazzu-Nascimento, T., Leão, P.A.G.C., Catai, J.R., Morbioli, G.G., Carrilho, E., 2016. Anal. Methods C 7312–7318.

Mendrick, D.L., Schnackenberg, L., 2009. Biomark. Med. 3, 605–615.

Nagy, B., Al-Rawhani, M.A., Cheah, B.C., Barrett, M.P., Cumming, D.R.S., 2018. ACS Sens. 3, 953–959.

Neumann, J.T., Sörensen, N.A., Schwemer, T., Ojeda, F., Bourry, R., Sciacca, V., Schaefer, S., Waldeyer, C., Sinning, C., Renné, T., Than, M., Parsonage, W., Wildi, K., Makarova, N., Schnabel, R.B., Landmesser, U., Mueller, C., Cullen, L., Greenslade, J., Zeller, T., Blankenberg, S., Karakas, M., Westermann, D., 2016. JAMA Cardiol. 1, 397–404.

Nicholson, J.K., Holmes, E., Kinross, J.M., Darzi, A.W., Takats, Z., Lindon, J.C., 2012. Nature 491, 384–392.

Piliarik, M., Sandoghdar, V., 2014. Nat. Commun. 5, 1–8.

Portsmann, B.B., Portsmann, T., Nugel, E., 1981. J. Clin. Chem. Clin. Biochem. 19, 435–439.

Puchades-Carrasco, L., Pineda- Lucena, A., 2017. Curr. Top. Med. Chem. 17, 2740–2751.

Purich, D.L., 2010. In: Enzyme Kinetics: Catalysis & Control. Elsevier, 215–285.

Rautela, G.S., Liedtke, R.J., 1978. Clin. Chem. 24, 108–114.

Rothwell, P.M., Giles, M.F., Chandratheva, A., Marquardt, L., Geraghty, O., Redgrave, J.N., Lovelock, C.E., Binney, L.E., Bull, L.M., Cuthbertson, F.C., Welch, S.J., Bosch, S., Carasco-Alexander, F., Silver, L.E., Gutnikov, S.A., Mehta, Z., 2007. Lancet 370, 1432–1442.

Roussos, B.G.G., 1967. Methods Enzymol. 12, 5–16.

Sreekumar, A., Poisson, L.M., Rajendiran, T.M., Khan, A.P., Cao, Q., Yu, J., Laxman, B., Mehra, R., Lonigro, R.J., Li, Y., Nyati, M.K., Ahsan, A., Kalyana-Sundaram, S., Han, B., Cao, X., Byun, J., Omenn, G.S., Ghosh, D., Pennathur, S., Alexander, D.C., Berger, A., Shuster, J.R., Wei, J.T., Varambally, S., Beecher, C., Chinnaiyan, A.M., 2009. Nature 457, 910–914.

Sullivan, L.B., Gui, D.Y., Heiden, M.G. Vander, 2016. Nat. Rev. Cancer 16, 680–693.

Sun, J.C., Beger, R.D., Schnackenberg, L.K., 2013. PerMed 10, 149–161.

Sunayama, H., Takeuchi, T., 2014. ACS Appl. Mater. Interfaces 6, 20003–20009.

Suzuki, M., 1981. J. Biochem. 89, 599–607.

Wang, L., Liu, S., Yang, W., Yu, H., Zhang, L., Ma, P., Wu, P., Li, X., Cho, K., Xue, S., Jiang, B., 2017. Sci. Rep. 7, 1–9.

Wang, Z., Klipfell, E., Bennett, B.J., Koeth, R., Levison, B.S., DuGar, B., Feldstein, A.E., Britt, E.B., Fu, X., Chung, Y.-M., Wu, Y., Schauer, P., Smith, J.D., Allayee, H., Tang, W.H.W., DiDonato, J.A., Lusis, A.J., Hazen, S.L., 2011. Nature 472, 57–63.

Washko, M.E., Rice, E.W., 1961. Clin. Chem. 7, 542–545.